in: Proc. 35th German Conference on Artificial Intelligence (KI 2012), Saarbrücken, Germany, LNCS 7526, pp. 85-96, Springer 2012

Avoiding Moving Persons by Using Simple Trajectory Prediction and Spatio Temporal Planning

Jens Kessler[1], Juergen Strobel[1], and Horst-Michael Gross[1]

Neuroinformatics and Cognitive Robotics Lab, Ilmenau University of Technology, 98693 Ilmenau, Germany

Abstract. If a mobile robot operates within its environment, it should take other persons into account while moving around. This work presents an approach, which predicts the movements of persons in a very simple way, and uses the predicted trajectories to plan a motion path for the robot. The presented motion prediction and planning process is much faster than real time. A potential field is applied to predict the person's movement trajectory, and a modified Fast Marching planner is used for the planning process. The aim of this work is, to create an early avoiding behavior of the robot, when the robot passes a person, to signal a "busy"'-behavior towards the person.

1 Introduction

In the near future, the application space of mobile robots will be more and more enhanced towards home environments, public care centers, and shopping malls. In these environments, the behavior of a robot should equal human behavior, especially when interacting with non-expert users. In experiments [12] it could be shown, that humans tend to observe complex technical devices, like a robot, as social entities. This causes the user to expect human-like behavior from a mobile robot.

When investigating human-robot interaction, the scenario of "a robot interacting with a person" is the most common use-case. In our work, we want to emphasize the case of human-robot interaction, when the robot does *not* want to interact with a person. For example, in nursing homes or hospitals, when the robot is on a tour to collect food orders or drives to the charging platform, an interaction with a randomly passing persons is not wanted. Interestingly, if humans do not want to interact with each other, the spatial configuration between these non-interaction partners signals the intention of each partner. Those spatial behavior patterns are quite complex and are profoundly investigated by psychologists. One aspect of spatial configurations and their meaning is described in the theory of the personal space, created by Hall [4]. In our work, we use the spatial configuration (or distance) which corresponds to "non interaction". We use a simple mathematical model of the personal space, and combine this model with the predicted motion of an observed person. With this knowledge, a non-intrusive path towards a predefined goal, which does not touch the personal space of a person, is planned.

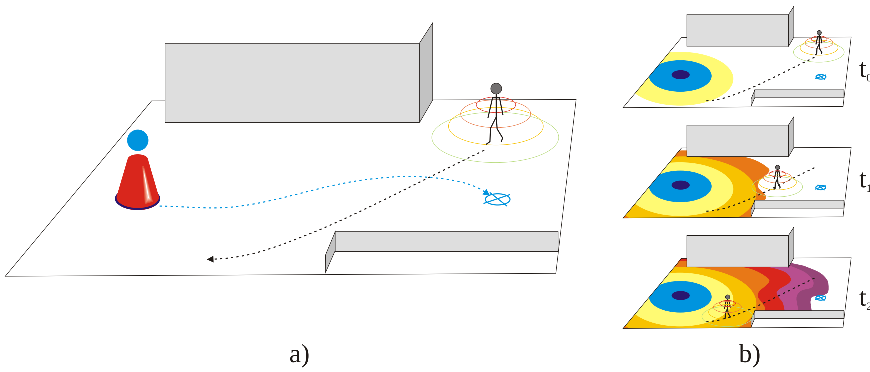

Fig. 1. The idea of the presented approach: the robot should be able to politely pass a moving person. To do so, the person path is predicted (see a)) and the personal space of the person is used in a spatio-temporal planning process to compute a feasible path. In b), a planning wave is propagated from the robot origin towards the goal (cross). This wavefront is deformed by the obstacles as well as the moving personal space from the predicted trajectory. When the goal is reached by the wavefront, the robot path could be extracted from calculated travel times.

Related work: A lot of work was done to investigate, if the model of the personal space, originally created from human-human interaction patterns, is also valid for human-robot interaction [2, 17]. Indeed, spatial configurations carry information about the intention of interaction partners, and are similar to the findings of Hall. The personal space is used regularly in robotic applications to solve tasks like approaching a person [8, 16] or path planning [15].

The benefit of the method of Svenstrup[16] is, to deal with changing person positions in a reactive way, but could get stuck in local minima due to the potential field motion control. The method of Sisbot[15] is only defined in an static environment, and does not consider time during the planning phase, so it could not incorporate moving persons. Anyhow, it uses the same simple personal space model than our approach. In [10], a rule based behavior was constructed to pass a person in a feasible distance in straight floors. Since this behavior was completely rule-based, it only works in floor-like environments and fails in unforeseen situations or environments, where the rules are not applicable. To our knowledge, there are no additional known publications on the topic of politely passing a moving person. However, there are many approaches which concern spatio-temporal path planning, which is a basic technique of our approach. The most advanced methods operate on planning trees. For example in [13, 9], lattice graphs are used to create a tree with spatial and temporal information, as long as the motion prediction of the moving objects are certain. In case of uncertain predictions, the algorithm only uses static spatial knowledge to plan further. This algorithm is very time consuming and is not processable in real time on a robot system. Another approach is presented by [6] and [8], where expanding random trees are used to create an collision free path in space and time to steer

in: Proc. 35th German Conference on Artificial Intelligence (KI 2012), Saarbrücken, Germany, LNCS 7526, pp. 85-96, Springer 2012

a robot. These approaches are very powerful in terms of describing the spatio-temporal information in state space, but fail when the robot deviates from the planned path in space or time. In such cases, large parts of the tree have to be re-calculated. In this work, a modified version of the Fast Marching planner [14] is used to enable the robot to find an optimal path, even when minor deviations from the optimal path occur. When incorporating moving objects into the spatio-temporal planning process, one fundamental precondition is a sufficient prediction of the motion trajectory of that object. It depends on the given task, to what time interval this prediction has to be useful. In our task, the motion trajectory is predicted in a duration of 10 seconds. A large set of prediction algorithms exist, mostly using probability densities, which are build upon a large set of trajectory observations [7, 1]. The disadvantage of these approaches is the need of an exhaustive data collection of trajectories over a long time. We prefer an out-of-the-box approach, where the trajectory of a person is predicted using the current motion direction and a potential field, presented in [6], to predict the person movement for the next few seconds.
Presented approach: A modified version of the Fast Marching Method (see [14]) is used to propagate a virtual traveling wave into the environment. The passing times of the wavefront through each point in space could be afterwards used to extract an optimal path. The passing time of the wavefront is determined by physical correct simulation of the wave. The travel speed in each point is directly related to the maximal driving speed of the robot, *and* the restrictions of traveling speed coming from the static and dynamic environment. The static restrictions are the obstacles. The dynamic restrictions of the environment are considered to come from the predicted motion trajectories of a person. A potential field method is used to predict the trajectory of the moving person. A brief overview of the key idea of the presented approach is shown in figure 1. The prediction method is described in detail in section 2, while the modified planning algorithm is presented in section 3. The paper is concluded by a set of experiments in section 4.

2 Prediction of the person's trajectory

In this section, the prediction of the person's trajectory is presented. A very simple, physically inspired model, also known as potential field, is proposed. This model is often used in robot navigation to avoid obstacles or approach a target, but here, it is used to predict near-future person movement for the next seconds. Note, that short time estimators, like the prediction step of a Kalman filter or the motion model of a particle filter, are not sufficient to predict a trajectory over several seconds. These approaches assume piecewise linear motion, like this approach also did, but the estimation is corrected by consecutive observations during each time step, which are not available on longer prediction periods. Our "correction" is done by the method of potential fields. The key idea is, to model the environment as a set of point like electric charges, which create an electrical field. This field could affect other charges by applying a force towards them. Two forces are modeled to predict the motion trajectory. First, the pushing force of obstacles is used to push a virtual person away to avoid collision. And second, the pulling force of an infinite virtual target line in front of the person is modeled to move the person forward. This line has a constant position, relative to the current person position. Next, a detailed description of the potential field model for an arbitrary configuration of charges is given.

2.1 The Potential Field

The presented approach uses two forces, which model the affected charges in different ways. The theoretical background, how charges could create a force, is identical in both cases. To calculate a force, coming from a generic set of charges at different positions $\boldsymbol{x_i}$, the electric field at a position $\boldsymbol{x}$ is defined as:

$$\boldsymbol{E}(\boldsymbol{x}) = \sum_{i=0}^{n} Q_i^- \cdot \frac{\boldsymbol{x} - \boldsymbol{x_i}}{|\boldsymbol{x} - \boldsymbol{x_i}|^3} \tag{1}$$

The resulting force on a negative charge is proportional to the vector $\boldsymbol{E}(\boldsymbol{x})$. To compute the pushing forces of the obstacles, a grid based world representation is used. If a cell contains an obstacle, a negative charge is defined there. A free cell does not contain any charge. The resulting vector of the electric field could be preprocessed in each free cell $\boldsymbol{x}_f$ by evaluating the obstacle cells in a circular neighborhood C of that cell.

$$\boldsymbol{E}_{obs}(\boldsymbol{x}_f) = \sum_{i=0}^{n} 1 \cdot \frac{\boldsymbol{x} - \boldsymbol{x_i}}{|\boldsymbol{x} - \boldsymbol{x_i}|^3} \ , \ (\boldsymbol{x}_i \in C(\boldsymbol{x}_f)) \cap (\boldsymbol{x}_i = obstacle) \tag{2}$$

The person itself is attracted by an infinite virtual line of positive charges. The position of that line is constant relative to the person. An example setting is shown in figure 2. This pulling field is defined by the infinite virtual target line L in front of the person, consisting of an *infinite* number of charges. Theoretically, the equation of the resulting vector could be formulated as:

$$\boldsymbol{E}_{target}(\boldsymbol{x}_f) = \int_{i=-\infty}^{\infty} -1 \cdot \frac{\boldsymbol{x} - \boldsymbol{x_i}}{|\boldsymbol{x} - \boldsymbol{x_i}|^3} d\boldsymbol{x}_i \ , \ \boldsymbol{x}_i \in L(\boldsymbol{x}_f) \tag{3}$$

If the line is always tangential towards the person's view direction, each point at line L could be paired with a corresponding (mirrored) point, where the sum of the corresponding field vectors directs towards the view direction. So, the final sum is an infinite number of vectors, pointing towards the view direction. Points, which are far away, apply nearly tangential forces, which are also very small, and so the sum of all these forces remains a finite number. Considering these facts, the resulting force from the tangential line could be *approximated* by a constant force in view direction of the person, where the strength is a parameter of the prediction algorithm. So, the overall resulting force is the vector sum of a force towards the current view direction, and a disturbing force, sourced by the obstacle configuration:

$$\boldsymbol{F}(\boldsymbol{x}) = Q^-(\boldsymbol{E}_{obs}(\boldsymbol{x}) + \boldsymbol{E}_{target}(\boldsymbol{x})) \tag{4}$$

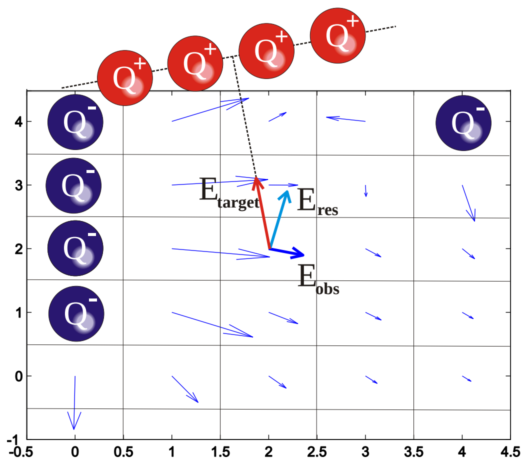

Fig. 2. This image shows the resulting vector field $\boldsymbol{E}_{obs}(\boldsymbol{x})$, which is sourced by the negative charges of the obstacle cells. The resulting force on the moving person is defined by two components. The pushing field E_{obs} of the obstacles and the pulling force E_{target} of the virtual target line. This results in a field vector E_{res}, which is proportional to the applied force.

Since the vector field $\boldsymbol{E}_{obs}(\boldsymbol{x})$ is only determined by the obstacle configuration, it could be processed off line. In such a way, the calculation of the resulting force $\boldsymbol{F}(\boldsymbol{x})$ is a very efficient operation.

2.2 Motion Prediction

The idea of predicting the trajectory is simply, to simulate the movement of a zero-mass, charged particle by considering the force $\boldsymbol{F}(\boldsymbol{x_j})$ in the currently predicted position $\boldsymbol{x_j}$, applied to the particle. Here, only the preprocessed static electric field is needed and a valid person position and walking direction of the person. A sufficient prediction of the person's trajectory for the next ten seconds could be provided by calculating the motion of the charged "person particle". If the motion of a charged particle within the resulting force field should be processed, the well known momentum equation could be used for that:

$$\begin{aligned} m \cdot \boldsymbol{v}_{t+1} &= m \cdot \boldsymbol{v}_t + \boldsymbol{F} \cdot \Delta t \\ \boldsymbol{v}_{t+1} &= \boldsymbol{v}_t + \boldsymbol{F}/m \cdot \Delta t \end{aligned} \tag{5}$$

Here, m denotes the mass of the charged particle, $\boldsymbol{v}_n$ denotes the speed at time n, and Δt is the time interval for one simulation step. It could be seen, that the mass influences the update of the speed. With a huge mass, the speed update is fairly slow and could lead to collisions. This changes, when the mass tends to small values, since than the speed tends to infinity and the speed vector tends to follow only the force vector $\boldsymbol{F}$. Since a collision free path of the person should be constructed, the particle should mainly react on the resulting force $\boldsymbol{F}$, and only an approximation of the momentum equation is used to update the current person speed:

$$\boldsymbol{v}_{t+1} = 0 + |\boldsymbol{v}_t| \cdot \frac{\boldsymbol{F}}{|\boldsymbol{F}|} \cdot \Delta t \tag{6}$$

It could be seen, that the mass of the particle is defined by $m = |\boldsymbol{F}|/|\boldsymbol{v}_t|$ and the speed direction of the previous motion step is not used. This assumption differs from a physical plausible approach. By re-defining the momentum equation,

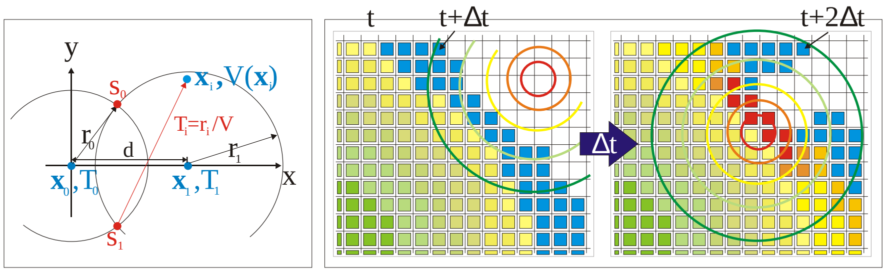

a) b1) b2)

Fig. 3. In image a), the details of the interpolation of one cell element of the wavefront are shown. They are described in detail in the text. On the right side b) a full simulation step is shown, where the personal space intersects the wavefront. Note, that only the marked elements of the wavefront are investigated for the current speed configuration. The wavefront is only updated with the current configuration until the elements reach the simulation time $t + \Delta t$, shown in b1). Afterwards, the personal space configuration is updated to $t + \Delta t$ and the propagation of the wave is executed, until $t + 2\Delta t$ is reached (see b2)).

only the direction of the person prediction is influenced by the potential field and the absolute value of the person speed is left constant. The trajectory of the moving person is calculated by sequentially applying equation 6. The predicted person's path is used for the robot's motion planning.

3 The Adapted Fast Marching Planner

The most common planning approaches [3, 5] use only binary values to encode cell traversability and have to create graphs from these binary information to compute optimal paths. In our approach, the Fast Marching Method from Setian [14] is used for robot path planning. It also operates on a regular grid. Each grid cell contains a cost value, that reflects the speed a wavefront is able to travel through this cell. Small values are assigned to cells, which should not be penetrated by the wavefront, like obstacles, whereas high values are assigned to free space and the wave can travel freely. Anyhow, all positive real values can be applied to the map cells, which is the major advantage of this planning method. Fast Marching computes to *which time* the wavefront crosses a cell. Our main idea is to calculate the cell crossing speed *at the time*, the cell is reached by the wavefront. This is the main difference to other approaches (e.g. E* [11]), where the travel speed of each cell is constant all the time. The benefit of the Fast Marching Method is the ability, to construct monotonical raising functions with *any* configuration of positive speed values, which is essential for a path planning algorithm to apply gradient descent for path following.

3.1 The Fast Marching Method

In the standard case, static velocity values are assigned for each cell, where free space is set to v_{max}, and near zero values are assigned to obstacle cells. The Fast Marching Method tries to find a numeric solution of the so called Eikonal equation $\boldsymbol{v}(\boldsymbol{x}) \cdot |\Delta T(\boldsymbol{x})| = 1$. The solution of this equation describes the evolution of a closed curve in time T, reacting on the different speeds $\boldsymbol{v}(\boldsymbol{x})$ at the positions $\boldsymbol{x}$. At most speed configurations, the solution could not be found in closed form. Fast Marching proposes a very simple numeric solution to solve this problem by sequntially interpolating small parts of the current wavefront to the next timestep. The "oldest" parts of the wavefront are propagated first. An expansion step is done by interpolating the wavefront for the current cell element $\boldsymbol{x}_i$ with the two neighboring elements with the smallest traveling times. For the interpolation of the cell element, the traveling times T_0, T_1 and positions $\boldsymbol{x}_0, \boldsymbol{x}_1$ of the two neighboring elements are considered. Also the current valid speed of that cell $v(\boldsymbol{x}_i)$ has to be known and is static for the standard case. In the first step, the positions $\boldsymbol{s_0}, \boldsymbol{s_1}$ of possible sources of the wavefront are calculated. Details of the geometric interpretation of the used values are sketched in figure 3 a):

$$\begin{aligned}
r_0 &= v(\boldsymbol{x}_i) * T_0 \\
r_1 &= v(\boldsymbol{x}_i) * T_1 \\
s_x &= (d^2 + r_0^2 - r_1^2)/2d \\
s_y &= \pm\sqrt{r_0^2 - s_x^2} \\
\boldsymbol{s_0} &= \langle s_x \ ; \ +s_y \rangle \\
\boldsymbol{s_1} &= \langle s_x \ ; \ -s_y \rangle
\end{aligned}$$

Here, d is the distance between $\boldsymbol{x}_0$ and $\boldsymbol{x}_1$ and defines the X-axis of the solution. As seen in figure 3a), there exist two possible sources $\boldsymbol{s}_0, \boldsymbol{s}_1$ of the wave origin to reach $\boldsymbol{x}_0$ in T_0 and $\boldsymbol{x}_1$ in T_1. The most distance source to our point $\boldsymbol{x}_i$ is chosen, since the point $\boldsymbol{x}_i$ would already have been interpolated if the nearest source is the correct one. With the correct source $\boldsymbol{s_j}$, the interpolation of the wave crossing time at position $\boldsymbol{x}_i$ is easy:

$$T_i = \frac{|\boldsymbol{x}_i - \boldsymbol{s}_j|}{v(\boldsymbol{x}_i)} \tag{7}$$

Note, that for very small values of the traveling speed, the passing time T_i will become very large and such elements are expanded very late in the propagation process. This is the case when the wave hits an obstacle cell, or the inner part of the personal space in our case.

3.2 Adaptation for Predicted Motions

To adapt the described interpolation method to time variant traveling speeds of $v(\boldsymbol{x_i}, t)$, a number of changes are necessary. First, the planning direction is reversed. In our case, the traveling times of the wave have the physical meaning, that the robot could actually cross that cell at the calculated passing time. So, the current robot position is the source of the wavefront. Setting the wave source to the initial robot position also helps to fuse the motion prediction with the planning process, since it is also known, at which time the person is at which position, and therefor the planning has to be applied *forward* in time.

Second, the fusion process is the fundamental change in wavefront propagation. The system starts from a time t_0 and updates the prediction of the person movement *as well as* the propagation of the wavefront in time intervals Δt. This means for the n-th planning step, that only those elements from the open list are expanded, whose travel times are smaller than $t_0 + n \cdot \Delta t$ and *only* for the expanded elements, the dynamic speed function $v(\boldsymbol{x_i}, t_0 + n \cdot \Delta t)$ is evaluated.

The dynamic speed function consists of two parts: the static part $v_{st}(\boldsymbol{x}_i)$ from the obstacle configuration, where the robot could drive in free space at a predefined speed (defined within each cell), and a dynamic part $v_{dyn}(\boldsymbol{x_i}, t_0 + n \cdot \Delta t)$, coming from the predicted motion trajectory of the person and their corresponding personal space:

$$v_{st}(\boldsymbol{x}_i) = \begin{cases} v_{max} \cdot \frac{d(\boldsymbol{x_i}) - d_{min}}{d_{max} - d_{min}} & , if \ d(\boldsymbol{x_i}) \leq d_{max} \\ v_{max} & , else \end{cases} \tag{8}$$

$$v_{dyn}(\boldsymbol{x}_i, t_0 + n \cdot \Delta t) = 1 - exp\left(\frac{|\boldsymbol{x}_i - \boldsymbol{x}_p(t_0 + n \cdot \Delta t)|^2}{2\pi\sigma_p^2}\right) \tag{9}$$

Here, $d(\boldsymbol{x_i})$ is the distance to the next obstacle cell, and $\boldsymbol{x}_p(t_0 + n \cdot \Delta t)$ is the predicted position of the person at the current simulation time. The personal space was defined by Hall [4] to be above 2.6 meters to symbolize non-interaction, and so, the value of σ_p is set to 2.6 meters. The fusion is done by a simple minimum operation:

$$v(\boldsymbol{x_i}, t_0 + n \cdot \Delta t) = min(v_{st}(\boldsymbol{x_i}), v_{dyn}(\boldsymbol{x}_i, t_0 + n \cdot \Delta t)) \tag{10}$$

Note, that high values of the personal space have not the same influence on the wavefront like obstacles, since the wave could travel very slowly through these cells. In this way, the wavefront travels around a person without touching the personal space, when enough free space is available. If the environments gets more narrow, the wave starts to travel through the personal space and the robot is allowed to penetrate that space without changing the algorithm.

3.3 Following the Calculated Path

The planning is complete, if the wavefront has reached the predefined target cell. Now, each cell passed by the wavefront contains a passing time, where the resulting driving path is calculated by gradient descent from the target towards the robot's original position. The robot has to follow this path as good as possible with the defined speeds, also calculated during the planning process. If the person deviates to much from the predicted path in space or time, a replanning has to be performed. This is done, if the Euclidean distance $|(x_p^{pred} - x_p^{obs}), (y_p^{pred} - y_p^{obs}), (t^{pred} - t^{obs})|$ is above a certain threshold.

4 Experiments and Results

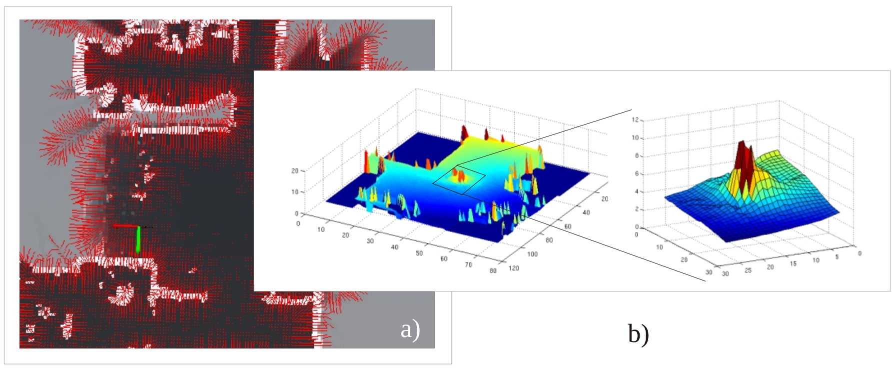

Fig. 4. In a), an example of the force field is shown, which is used for motion prediction. In b) the navigation function of the passing times of the wave from the wide space scenario is shown. The traveling time raises, when the wavefront hits the personal space of the person during planning. A detailed view of that part of the function is shown on the right.

In our experiments two typical scenarios with different characteristics where evaluated. At the one hand, we evaluated the planning and prediction process regarding the quality of the path, and at the other hand, we evaluated the processing time, needed to create the path. The scenarios should only present a preliminary test of the feasibility of our method and do not present a full experimental coverage.

The first scenario tests a passage with narrow space in our living lab. Here, a person moves on a straight line, and the robot has to cross this line by taking into account the currently measured walking speed of the person. In the second scenario, the person meets the robot in a wide corridor. The person moves also in a straight line and the robot should approach a goal behind the person by driving in the opposite direction. Here, the person should move directly towards the robots original position and the robot has to avoid the person. Both scenarios use the map of our lab for planning. The map has a resolution of 10cm per cell. The resulting planning function and the associated cell speeds, which correspond to the passing time of the wavefront, are shown in figure 5 for the narrow space scenario and figure 6 for the wider space passing scenario. It can be seen, that in both cases the personal space of the moving person slows down the wavefront

in: Proc. 35th German Conference on Artificial Intelligence (KI 2012), Saarbrücken, Germany, LNCS 7526, pp. 85-96, Springer 2012

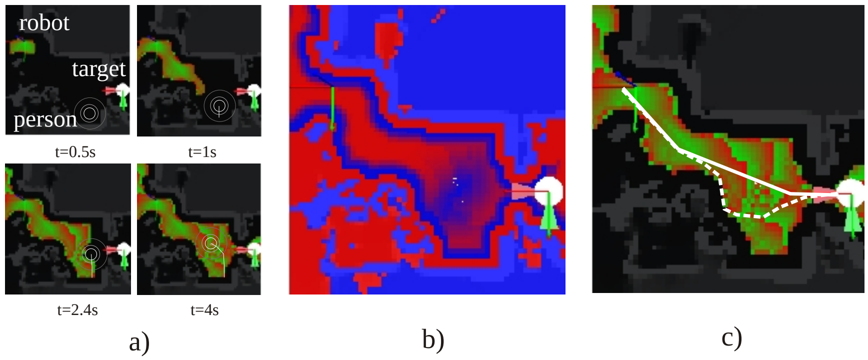

Fig. 5. In part a): snapshots of the propagation of the wavefront in a narrow passage. The robot starts on the left side and has to reach the goal on the lower right. The person is located at the bottom (circles) and crosses the path of the robot. Note, that every second in simulation time the color of the wavefront changes from red to green to visualize the form of the wavefront. Part b) shows the calculated travel speed, the robot should drive upon traveling through each cell. Dark blue values mean very slow speeds while light red values indicate the maximal allowed speed. In part c) the final path with avoiding behavior is shown as a dashed line, while the original path, without a person being present, is shown as a solid line.

and guides the wavefront around the person. When the goal is reached by the wavefront, gradient descent is used to extract the optimal path. Figures 6 c) and 5 c) also show the planning results, when no person is present.

To enable the robot to react on person movement, it should be able to plan the path much faster than real time. In fact, it must be possible to plan the path in a fraction of a second for multiple seconds beforehand. If not, the person has moved already when the path is calculated, and the estimation is not valid anymore at the time the robot starts moving.

We measure the average runtime of the algorithm with different prediction intervals Δt for a total prediction period of 10 seconds. Smaller time intervals Δt mean more accurate motion prediction and wave propagation. Table 1 shows the results of the runtime investigation. In average, the method is capable of predicting and planning 13 times faster than real time. We chose a simulation interval of 0.5 seconds for the motion prediction and the update of the planning function, since this time provides good accuracy by providing still good performance. The prediction and planning of ten seconds of motion can be done in 770 milliseconds.

The calculation of the force field $\boldsymbol{E}_{obs}$ is constant for the given map and is done once before the algorithm starts. Since this is a time consuming operation, it took 10.3 seconds for the given map of the lab to build the vector field. For the experiments a standard dual core mobile processor with 2.1 GHz was used. Only one core does the wavefront propagation since this is a highly sequential task and it is hard to parallelize this algorithm.

in: Proc. 35th German Conference on Artificial Intelligence (KI 2012), Saarbrücken, Germany, LNCS 7526, pp. 85-96, Springer 2012

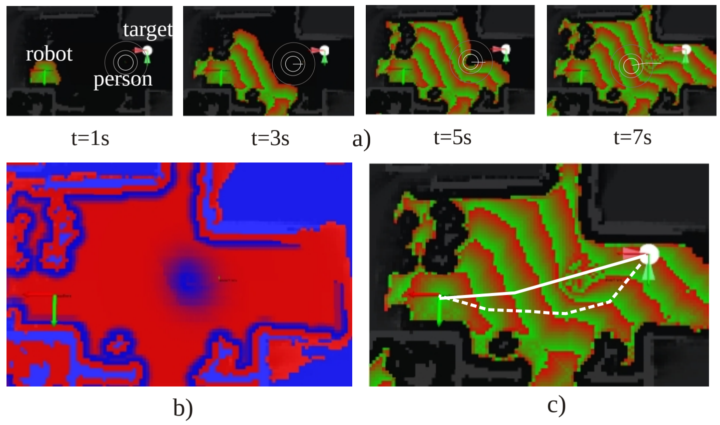

Fig. 6. Here, the wide space scenario is shown, where the person heads directly towards the robot original position and the robot has to avoid the person, since the robot's target lies behind the person. For a full description of a), b), and c), please refer to figure 5.

Simulation Step	**Δt=3s**	**Δt=1.5s**	**Δt=0.5s**	**Δt=0.2s**
t_{avg}	75ms	75ms	75ms	89.2ms
t_{σ}	72ms	35ms	18ms	13.4ms
Speed factor	13	13	13	11

Table 1. Overview of the resulting computation times for different prediction intervals Δt for the person's trajectory prediction and wave propagation. Here, t_{avg} is the average computation time, while t_{σ} is the variance of the computation time per iteration step. On prediction steps up to 0.5 seconds, the system is able to predict and plan 13 times faster than real time. Only on small simulation steps, this factor begins to fall. In our scenario tests, a simulation time step of 0.5 seconds is chosen.

5 Conclusion and future work

In this work, an approach for spatio-temporal path planning with regard of one moving person is shown. The main benefit is the possibility to create a path under all circumstances. If possible, the robot avoids the personal space of a person, when there is enough space. If not, the robot at least slows down. At the one hand, this behavior of the robot has to be investigated in further experiments. At the other hand, an investigation has to be done, what happens if the robot could not keep track of the planned path and planned time and deviates from the given task.

Acknowledgment

This work was financed by the project AAL-2009-2-049 "Adaptable Ambient Living Assistant" (ALIAS) co-funded by the European Commission and the Federal Ministry of Education and Research (BMBF) in the Ambient Assisted Living (AAL) program.

References

1. A. Bruce and G. G. Gordon. Better motion prediction for people-tracking. In *Proc. ICRA*, 2004.
2. K. Dautenhahn et al. How may i serve you? a robot companion approaching a seated person in a helping context. In *Proc. HRI*, pages 172–179, 2006.
3. E.W. Dijkstra. A note on two problems in connexion with graphs. *Numerische Mathematik*, 1:269–271, 1959.
4. E.T. Hall. *The hidden dimension.* Doubleday, NY, 1966.
5. E.P. Hart, N.J Nilsson, and B. Raphael. A formal basis for the heuristic determination of minimum cost paths. *IEEE Transactions on Systems, Science and Cybernetics*, 4:100–107, 1968.
6. F. Hoeller, D. Schulz, M. Moors, and F.E. Schneider. Accompanying persons with a mobile robot using motion prediction and probabilistic roadmaps. In *Proc.IROS*, pages 1260–1265, 2007.
7. T. Kanda, M. Shiomi, Z. Miyashita, H. Ishiguro, and N. Hagita. A communication robot in a shopping mall. *IEEE Transactions on Robotics*, 26(5):897–913, 2010.
8. J. Kessler, A. Scheidig, and H.-M. Gross. Approaching a person in a socially acceptable manner using expanding random trees. In *Proc. ECMR*, pages 95–100, 2011.
9. M. Likhachev and D. Ferguson. Planning long dynamically-feasible manuevers for autonomous vehicles. *Int. Journal of Robotics Research*, 28(8):933–945, 2009.
10. E. Pacchierotti, H.I. Christensen, and P. Jensfelt. Evaluation of passing distance for social robots. In *Proc. RO-MAN*, 2006.
11. R. Philippsen. *Motion Planning and Obstacle Avoidance for Mobile Robots in Highly Cluttered Dynamic Environments, PHD Thesis.* Univ. of Toulouse, Ecole Polytechnique Federale de Lausanne, 2004.
12. B. Reeves and C. Nass. *The Media Equation: How People Treat Computers, Television, and New Medial Like Real People and Places.* CSLI Press, Stanford, 1996.
13. M. Rufli and R. Siegwart. On the application of the d* search algorithm to time-based planning on lattice graphs. In *Proc. ECMR*, pages 105–110, 2009.
14. J.A. Sethian. A fast marching level set method for monotonically advancing fronts. *Proc. Nat. Acad. Sci.*, 93(4):1591–1595, 1996.
15. E.A. Sisbot. *Towards Human-Aware Robot Motions, PHD Thesis.* Univ. of Toulouse, Toulouse, 2006.
16. M. Svenstrup, S. Tranberg, H.J Andersen, and T. Bak. Pose estimation and adaptive robot behaviour for human-robot interaction. In *Proc. ICRA*, pages 3571–3576, 2009.
17. L. Takayama and C. Pantofaru. Influences on proxemic behaviours in human-robot interaction. In *Proc. IROS*, pages 5495–5502, 2009.